23rd ABCM International Congress of Mechanical Engineering
December 6-11, 2015, Rio de Janeiro, RJ, Brazil

# EVALUATION OF SHOCK ABSORBER TESTING METHODOLOGY THROUGH NUMERICAL SIMULATION

**Guilherme Barbosa Lima**
Universidade Federal de Minas Gerais - UFMG
blima.guilherme@gmail.com

**Bruna Luiza Nolli**
Universidade Federal de Minas Gerais - UFMG
nolli.bruna@gmail.com

**Ana Thaís Almeida de Melo**
Universidade Federal de Minas Gerais - UFMG
melo.atm@gmail.com

***Abstract.*** *Shock absorbers are used in oscillatory systems in order to control vibration, dissipating the motion energy. To predict shock absorbers behavior in the system, it is necessary to know its characteristics. However, the details of the shock absorber setup are usually restricted to the manufacturer, leading to the need of testing the equipment. Previous studies described test methodologies in which it is measured the displacement, velocity and reaction forces during its actuation with a cyclical test machine. This testing main goal is to decompose the measured force in the theoretical portions, isolating the interest variables. Some variables are velocity dependent and others are only displacement dependent, requiring a proper definition and control of the test velocity to allow the isolation of force components. In this study an experimental test methodology was evaluated through a numerical simulation of a shock absorber's simplified model, in order to determine the tests boundary conditions that allow the measured force decomposition. The model was developed for a hydro-pneumatic shock absorber (viscous damping and gas charged), representing the theoretical forces acting on it: damping, stiffness and Coulomb friction. The simulation results had a good agreement with the theoretical data and revealed the ideal testing boundary conditions, defining mainly the actuating velocity along shock absorber axis.*

***Keywords:*** *shock absorber, testing methodology, numerical simulation.*

## 1. INTRODUCTION

The first vehicles had no suspension system, and the wheels were rigidly fixed on the chassis. All the vibration caused by ground was transmitted to the cockpit, making the ride uncomfortable for the passengers, dangerous to the payload, and unsafe to the vehicle's integrity. The concept of suspension was introduced in order to reduce the vibration, using at first only springs and then shock absorbers. Therefore, the mechanical energy of sprung mass would be dissipated and the vehicle would oscillate in a controlled way, in a shorter period of time and with less intensity.

Vehicle's application is the most important aspect for the design of suspension systems. It can be designed focusing on maximize the tire-ground contact, to improve the passenger's comfort, to increase the directional stability, or to absorb the impact of jumps and low frequency obstacles, in off-road applications. Most often, the objectives are achieved through suspension constant's setting: stiffness and damping. Thus, the characterization of springs and shock absorbers are important to achieve the proposed performance and to reduce the experimental calibration time.

Stiffness, which comes from the spring, is defined through its geometrical parameters, and for pneumatic springs the thermodynamics laws about pressure variation on gas under compression are used. When shock absorber's damping is by friction, this is a function of normal forces and friction coefficient. When damping is viscous, the constant is proportional to the relative velocity.

Damping constant of hydraulic shock absorbers is more complex to be determined. The energy dissipation occurs through the flow of viscous fluid by valves with orifices. Thereby, the fluid is heated by the changes on the system's energy: mechanical energy on the spring and on the sprung mass is converted in kinematic energy of shock absorber, and then converted as thermal energy. This action heats the fluid and the shock absorber's body, which dissipate energy to the atmosphere. Difficulties in determining all the shock absorbers characteristics for a mathematical model makes experimental tests necessary.

According to Dixon (1999) the easiest form to perform tests on shock absorbers is using an electro-mechanic machine with a crank-slider mechanism. This test device allows the use of several velocities and strokes, control of the electric motor power source and changing the crank's effective radius, respectively. This way the test can be performed in all speed and force range, important to have a complete characterization of a shock absorber.

Lima (2014) performed tests with an equipment with the same characteristics and developed a methodology for obtain shock absorber's data. Supported by the mathematical model of a shock absorber proposed by Dixon (1999), Lima (2014) established measurement criteria to find each one of the force's fraction of damping reaction, but the force from the gas could not be observed without the damping force's influences. Lima (2014) found faults on the testing device that led to the errors on the data acquired, as the equipment could not reach all the boundary conditions the drive system had to perform, as described on the methodology proposed by Lima (2014).

Thereby, the objective of this study is to develop a numerical simulation of a shock absorber working together with test device, using system's variables and constants based on reliable results of Lima (2014), to predict the shock absorber's behavior during tests, show differences between the expected and obtained results and determine the ideal boundary conditions to realize the experimental tests.

## 2. METHODOLOGY

The numerical simulations of the test procedures required the mathematical model of both mechanisms, the drive and the shock absorber, in order to allow a direct comparison between the results of test, obtained by Lima (2014) and of simulation, presented in this paper. Besides, the results obtained in simulation will determine the ideal boundary conditions for future testing.

The drive's model was developed based on the testing device used by Lima (2014), showed on Fig. 1, and the shock absorber's model was based on a hydraulic, monotube, gas charged type, as the model shown on Fig. 2.

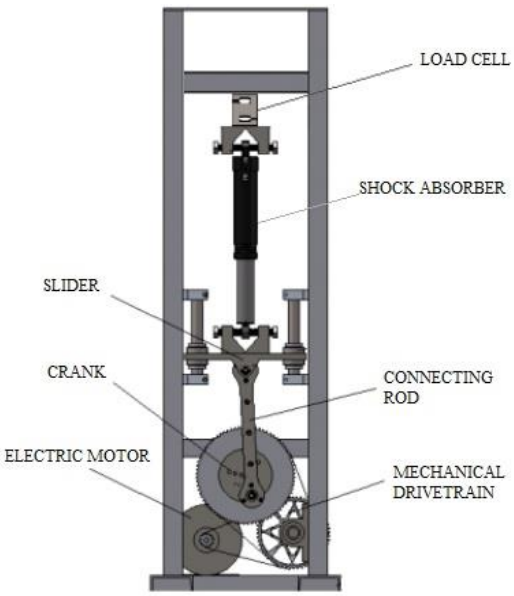


Figure 1. Test device. (Lima, 2014 – adapted)

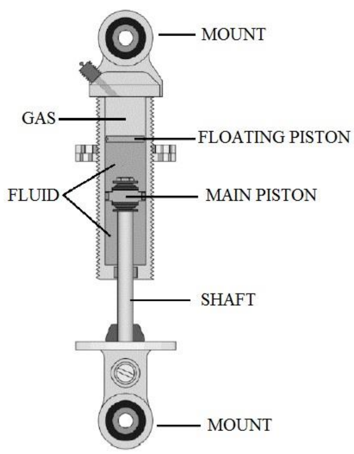


Figure 2. Monotube, gas charged shock absorber. (Thede, 2010 – adapted)

### 2.1 Test device's mathematical modelling

A robust metal structure holds all the components of the test device used by Lima (2014). It has an electric motor connected to a frequency converter, a gear train to increase the torque, and a crank-slider mechanism. The shock absorber has one end fixed at the metal structure, and the other end moves cyclically with the crank-slider system.

At the crank-slider mechanism, the slider's position defines shock absorber's displacement and it is a function of crank`s rotation angle; and slider's velocity, which is a function of crank`s angular velocity, gives shock absorber's speed. Both shock absorber's displacement and velocity can be calculated using Eq. 1 and Eq. 2. In this equations, $x_c$ is the slider's displacement, $v_c$ is the slider's velocity, $r$ is the crank's effective radius, $b$ is the connecting rod's length and $w$ is the crank's angular velocity.

$$x_c = r.\cos(w.t) + (b^2-r^2.\sin^2(w.t))^{1/2} - (b^2-r^2)^{1/2} \qquad (1)$$

$$v_c = -r.w.\sin(w.t).(1+(r.\cos(w.t)/(b^2-r^2.\sin^2(w.t))^{1/2})) \qquad (2)$$

The test device's drive system is composed by a frequency converter acting on the electric motor in order to control its speed. This action maintains the crank's angular velocity constant, as the crank and motor are connected through a mechanical drivetrain.

The frequency converter is used to keep electric motor's velocity constant independent of shock absorber`s reaction force. Hence, the only data used to feed the drive mechanism's mathematical model is the angular velocity of crank. With this information is possible to obtain the slider`s displacement, and deriving it, the slider`s speed is calculated.

### 2.2 Shock absorber's mathematical modelling

The shock absorber model used by Lima (2014) is hydraulic, it is a monotube type, and it has a gas charge, which is separated from the fluid through floating piston. The movement between shock absorber parts creates a motion among the main piston and the working fluid. The main piston has orifices to restrict the fluid flow, so while it drains, its kinematic energy is converted to heat due to viscosity effects.

Cavitation is a phenomenon that converts the working fluid into vapor and decreases the shock absorber's performance. This happens while the fluid drains trough the piston, and a major variation on the internal pressure happens, which could cause the fluid pressure to get lower than its vapor pressure. To avoid this phenomenon, the shock absorbers are loaded with a pressurized gas, therefore the fluid is always subject to a minimum pressure, higher than its vapor pressure.

At the test device used by Lima (2014), the load cell was installed between the shock absorber and the metallic structure because Dixon (1999) affirms that with this configuration the load cell will not measure the inertial force of the system. In case of installing the load cell between the shock absorber and the slider, all the inertial forces, produced by the drive mechanisms inertia, will be transferred through the load cell. The force acquired by the load cell during the test, $F_D$, is given by Eq. 3, and $F_D(v)$ is the portion of the force dependent of velocity, $F_D(x)$ is the portion dependent on displacement, $P$ is the weight held by the structure, $F_G$ is the gas static force, and $F_F$ is the friction force.

$$F_D = F_D(v) + F_D(x) + P + F_G + F_F \qquad (3)$$

The value of the weight held by the structure ($P$) is much lower than the forces inside the shock absorber ($F_D(x)$, $F_D(v)$, $F_G$, $F_F$ ), and it can be eliminated offsetting the value measured by the load cell. So, in this paper this load was neglected.

To represent the forces in its correct directions, it was adopted the following signal criteria: the full extended shock absorber (initial state) has null displacement, increasing as it is compressed; the compression velocity is positive and the extension is negative; and as the compression velocity is positive and the damping force is opposite to the movement, it was defined that all the forces acting against the compression are negative. This way, the gas force is always positive, as it is acting in sense of extending the shock absorber, the friction and damping forces, which are always against the movement, on compression are negative and on extension are positive.

#### 2.2.1 Velocity dependent force ($F_D(v)$)

According to Dixon (1999), the simplest shock absorber to be modeled is the linear one, which has the damping force linearly dependent of velocity. As the shock absorber used by Lima (2014) had different behaviors for compression and extension, it was chosen to use a bilinear model, with the compression velocity proportional to compression and extension velocity proportional to extension, both with different values. Equation 4 shows the linear dependence between damping force ($F_D(v)$) and velocity ($v_c$), and $c$ is the damping constant.

$$F_D(v) = c.v_c \tag{4}$$

At Fig. 3 can be observed the typical curve for bilinear shock absorbers.

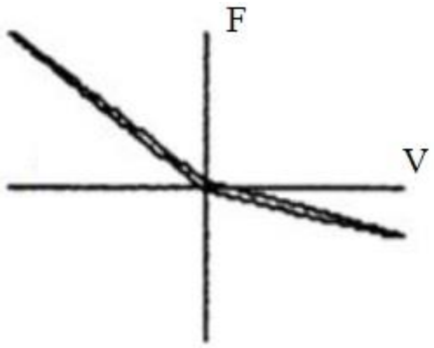


Figure 3. Typical curve of a bilinear shock absorber. (Dixon, 1999 – adapted)

### 2.2.2 Displacement dependent force ($F_D(x)$)

The displacement dependent force occurs due to the variation of the gas pressure inside the shock absorber, in accordance with Dixon (1999). This gas main goal is to avoid cavitation phenomenon.

The gas compression is due to fluid volume variation caused by the entrance of the shaft inside the shock absorber's body. When this occurs, the gas compress to keep internal volume, producing a force (always positive) to expel the shaft.

Floating piston displacement is retrieved through shaft displacement and ratio between shaft and piston areas. Equation 5 defines piston displacement, $D_P$, as a function of shaft displacement, $D_S$, of the shaft area, $A_S$, and of piston area, $A_P$.

$$D_P = D_S \, . \, (A_S / A_P) \tag{5}$$

The piston displacement causes the gas to compress, which can be considered an adiabatic polytrophic compression, as mentioned in both Lang and Sonnenburg (1995) and Çengel and Boles (2001) works. In general the gas used in shock absorbers is nitrogen, leading to the use of its thermodynamic properties, in order to calculate the pressure variations.

The floating piston's displacement is converted in displaced volume, and then in variation of gas' pressure. This process occurs iteratively through Eq. 6, in which $P_2$ is the pressure at the iteration's end, $P_1$ is the initial pressure (whose value is known), $V_1$ is the initial volume occupied by gas, $V_2$ is the final volume after the piston's displacement, and $k$ is the nitrogen's polytrophic constant.

$$P_2 = P_1.(V_1/V_2)^k \tag{6}$$

As the initial pressure is modelled in this stage, the force $F_G$, caused by the initial pressure in accounted in model without the addition of a new force.

### 2.2.3 Friction force ($F_F$)

A tight adjustment between the sealing components is necessary to avoid fluid and gas to scape, and because of the requirement of sealing between chambers. This force is a Coulomb friction force, and acts like the damping force, it is always on the opposite direction of the movement, and it is independent of position and velocity of shock absorber. This force just depend of the normal forces acting on the surfaces in contact with the sealing components, so in this paper it was consider constant with a value of 50 N, based on considerations obtained by Lima (2014).

## 2.3 Model's combination

From the modelling of all elements of testing device and shock absorber, it was possible to unite the models and simulate the test performed by Lima (2014). The model's input data were the components geometry, which remains unchanged, and the electric motor rotational velocity, which was altered due to determination of force's behavior in each condition.

Figure 4 presents the simulated system's block diagram, highlighting the drive mechanism and the calculation of each of the forces.

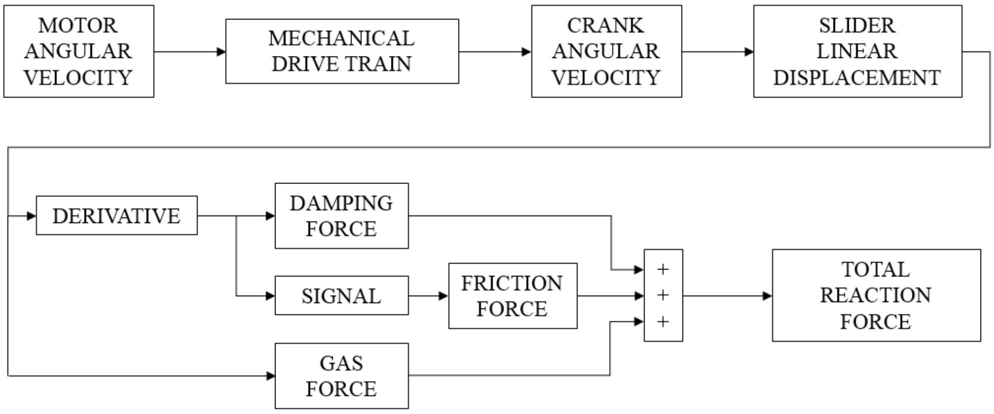


Figure 4. System's block diagram.

## 2.4 Numerical simulation methodology

At the methodology proposed by Lima (2014), the shock absorber test happened in two stages. In the first one the shock absorber was driven at a maximum velocity of 540 mm/s and the reaction force was acquired. This force has three components: damping, friction and gas forces. In the second stage the same procedure occurs at a maximum speed of 10 mm/s. Because of the low velocity, the damping force, proportional to speed, do not act, and the reaction force measured has only two components: friction and gas forces. So, in order to obtain the damping force it is just subtract the result from the first part of the test of the result of the second one.

In order to be able to compare the results, the same methodology used by Lima (2014) was applied in the simulation.

At first, the model was simulated for the maximum displacement and velocity of 100 mm and 500 mm/s, respectively, as it was proposed by Lima (2014). Then the simulation occurs for a maximum speed of 10 mm/s for the shock absorber. The total reaction force was compared to gas and friction forces to determine if the velocity used in the second part of the test was slow enough to eliminate the damping force. In case of this force is not eliminated, the last part of the simulation would determine the velocity that makes the damping force so small to be neglected.

## 3. RESULTS

The first result of interest was the comparison between the total reaction force, obtained through simulation, and the force experimentally measure by Lima (2014), in order to confirm that the simulation represents the tests performed.

Figure 5 presents the force as a function of displacement and velocity for the testing performed by Lima (2014), and Fig. 6 presents the same curves obtained from simulation.

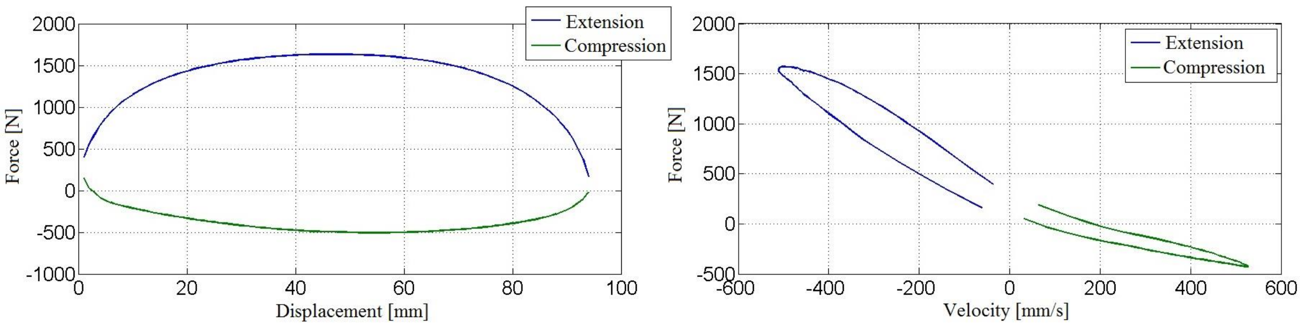


Figure 5. Force vs. displacement and force vs. velocity curves obtained by Lima (2014). (Lima, 2014 – adapted)

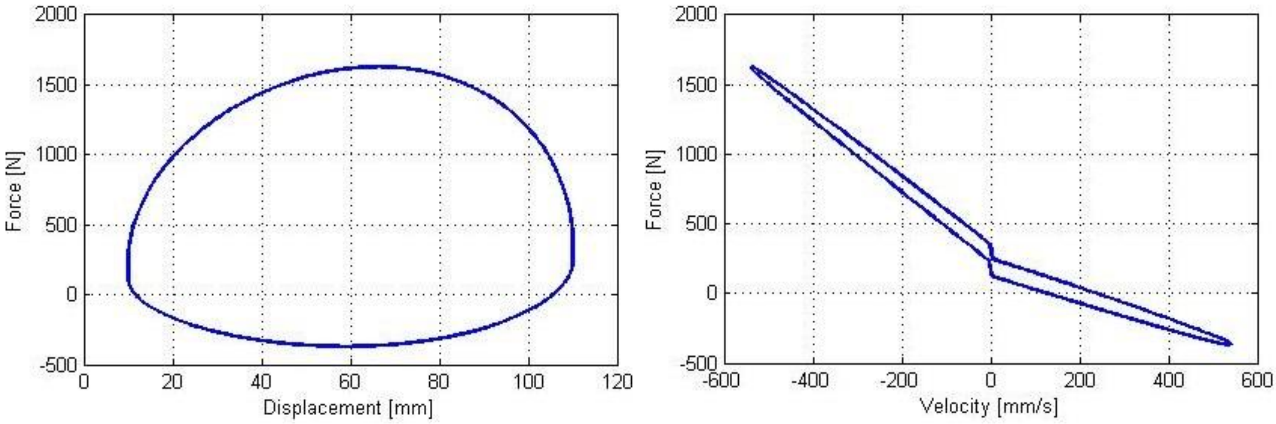


Figure 6. Force vs. Displacement and force vs. velocity curves obtained in system's simulation.

Comparing both curves in the same domain (displacement or velocity), it was possible to affirm that even having small differences in numeric values, the behavior of curves was the same. As Lima (2014) could not determine precisely the damping constant and the gas reaction force, the values used in simulation were estimates, introducing an error on the calculations.

Figure 7 shows the total reaction force, plotted with all its components, as a function of velocity. Even the gas and friction forces not being a function of velocity, or the damping force not being a function of displacement, this analysis could be made in both domains, as the drive mechanism has its velocity dependent from displacement. The comparison was chosen to be made in the velocity domain because this was the only change between all the simulations presented in this paper and in the tests performed by Lima (2014).

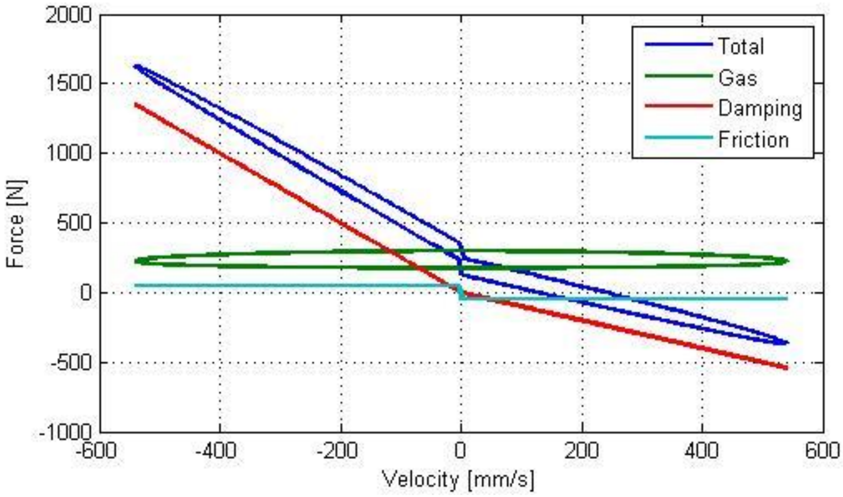


Figure 7. Total reaction force of shock absorber decomposed in its components.

On Fig. 7 it is possible to observe the behavior of each one of the three forces. The damping force presents itself in a bilinear form, with different inclinations for both compression and extension, as the proposed model. It also has the opposite signal from the velocity, indicating that the force acts against the movement. The same consideration can be observed in the friction force. The gas force is also befitting the model proposed, its maximum and minimum values occur in zero velocity, which are the extremes of movement, with the shock absorbers full compressed and full extended, respectively.

As it can be observed from Fig. 5 and Fig. 7, the force obtained by Lima (2014) resembles with the total force obtained in simulation, in other words, without exclude the gas and the friction. The curve's shape, like a cycle, and the offset from zero, is due to the gas portion, which can be clearly seen on Fig. 5.

It was explained that in order to measure only the gas and friction forces, the maximum velocity to be applied on the shock absorber was settled to be 10 mm/s. This velocity was determined arbitrarily, without references to support this value.

Due to the drivetrain characteristics, the minimum velocity the test device could reach was 40 mm/s without instability on the velocity. In lower velocities the equipment presented instability in control systems, preventing the test's repeatability.

Considering this limitation, the simulation was set to achieve a maximum velocity of 40 mm/s. The results of this simulation are presented on Fig. 8.

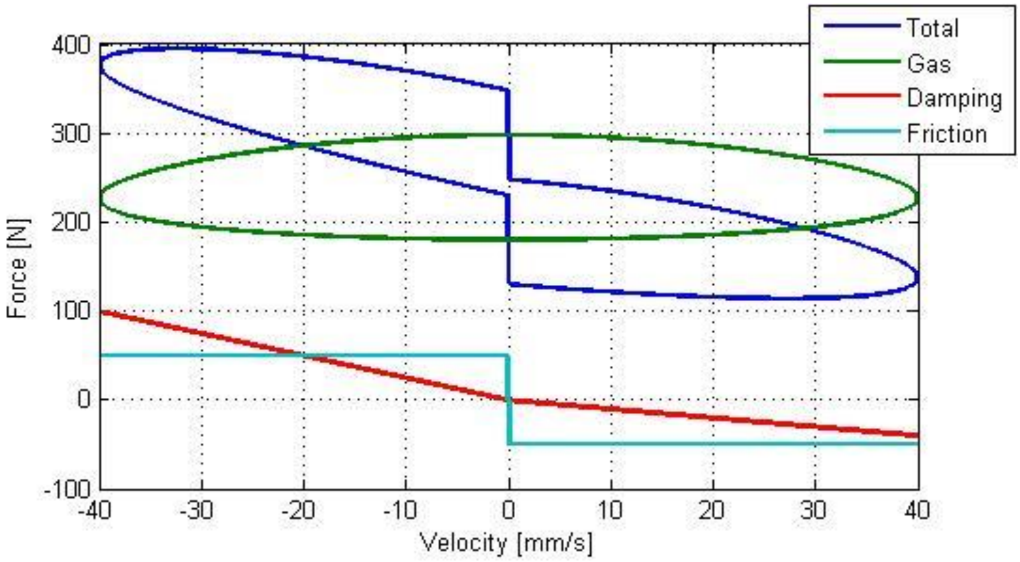


Figure 8. Force vs. velocity curve for a maximum velocity of 40 mm/s.

As it can be seen on Fig. 8, the portion that refers to the damping force represents approximately 25% of the total reaction force. For Lima's methodology (2014) to succeed, in this situation the damping force should be small enough to be neglected.

Considering that the test equipment could reach the desired velocity of 10 mm/s, the simulation was performed for this condition, and its results are presented on Fig. 9.

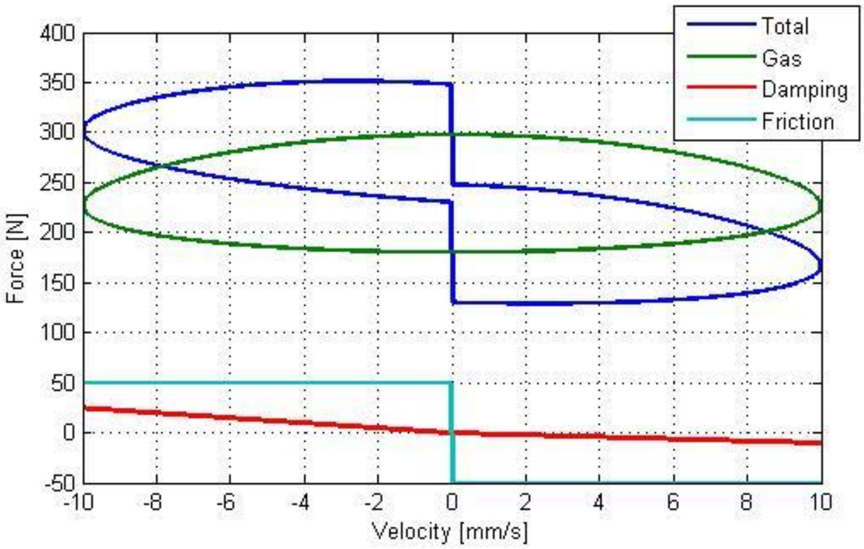


Figure 9. Force vs. velocity curve for a maximum velocity of 10 mm/s.

In this situation, the damping force represents about 8.5% of the reaction force, but comparing it to the friction force, the difference is about 50%. As the friction force is one of the most important portions on this step, an error that is 50% of its value is large enough to make the velocity of 10 mm/s inadequate to be used to determine the gas and friction forces.

As the methodology proposed by Lima (2014) had not obtained the desired results, the model was used to define a new value of speed that will allow the proper decomposition of the forces inside a shock absorber. Then the numeric model was simulated with different values of speed in order to find the most suitable one. The main goal was to produce a damping force that could be neglected.

Figure 10 presents the results of numeric simulation considering a maximum velocity of 3 mm/s, which was the point that the damping force represents 3% of total reaction force and less than 10% of the friction force, at its most influent point, the maximum extension speed.

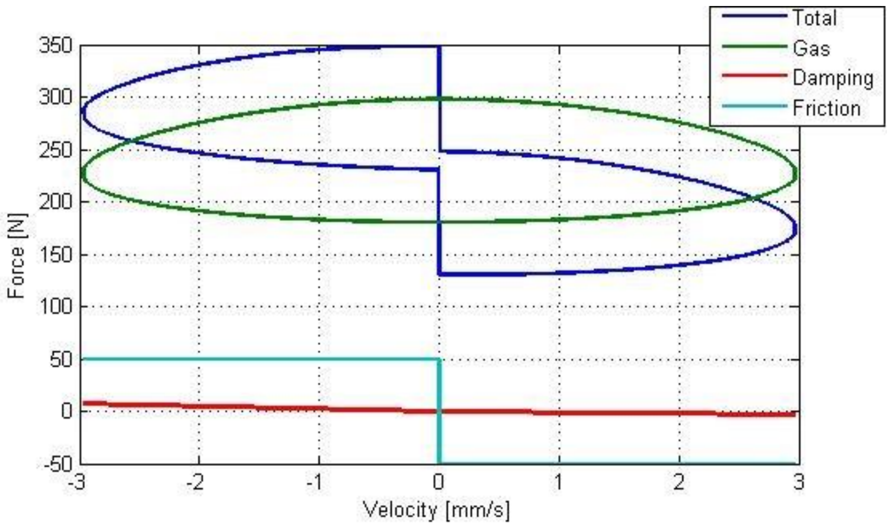


Figure 10. Force vs. velocity curve for a maximum velocity of 3 mm/s.

At this speed, the force splitting method, proposed by Lima (2014), would be possible to be executed with a minimum of error produced, probably smaller than the global measurement error. This way all three portions would be measured individually and the shock absorber behavior would be completely mapped.

This condition, in which the damping force presents a negligible value, requires a possible problem for the test device's drive system, as it requires to the electric motor to drive the system with about 6 rpm, which is less than 0.3% of the motor's nominal velocity. The electric motors in general are not designed to run at a low velocity like that and it will require a special control system to be able to drive the system.

## 4. CONCLUSIONS

After the simulation of the complete system, it was noticed that this system can be considered a good representation of the test performed by Lima (2014), as it was shown in the comparison between the results of testing and simulation.

It was clear that the results obtained by Lima (2014) had an error induced by the damping force that was not negligible at the step of determination of gas and friction forces. This error certainly influenced on the force split method.

For the testing velocities proposed, 10 and 40 mm/s, the damping force was still a significant percentage of the reaction force, which made the results affected by its presence.

For the velocity determined by the simulation results, 3 mm/s, outcomes in less than 3% of the reaction force, leading to the results desired in the testing methodology. In this condition the electric motor will have to operate in an extremely low velocity (0.3% of nominal value) and may require an additional control system in order to allow this operational condition.

## 5. REFERENCES

Çengel, Y.A., and Boles, M.A., 2001. *Thermodynamics: an engineering approach*. McGraw-Hill, Boston, 6th edition.

Dixon, J.C., 1999. *The shock absorber handbook*. SAE, Warrendale.

Lang, R., Sonnenburg, R., 1995. "A detailed shock absorber model for full vehicle simulation". In *MSC Adams Conference*. Detroit, USA.

Lima, G.B., 2014. *Caracterização experimental do comportamento dinâmico de amortecedores hidropneumáticos*. Final course assignments, Universidade Federal de Minas Gerais, Belo Horizonte.

Thede, P., Parks, L., 2010. *Racetech's motorcycle suspension bible*. Motorbooks, Minneapolis.

## 6. RESPONSIBILITY NOTICE

The authors are the only responsible for the printed material included in this paper.